Development 134, 4273-4282 (2007) doi:10.1242/dev.010397

A wave of EGFR signaling determines cell alignment and intercalation in the *Drosophila* tracheal placode

Mayuko Nishimura[1,2], Yoshiko Inoue[1,*] and Shigeo Hayashi[1,2,†]

Invagination of organ placodes converts flat epithelia into three-dimensional organs. Cell tracing in the *Drosophila* tracheal placode revealed that, in the 30-minute period before invagination, cells enter mitotic quiescence and form short rows that encircle the future invagination site. The cells in the rows align to form a smooth boundary ('boundary smoothing'), accompanied by a transient increase in myosin at the boundary and cell intercalation oriented in parallel with the cellular rows. Cells then undergo apical constriction and invaginate, followed by radially oriented mitosis in the placode. Prior to invagination, ERK MAP kinase is activated in an outward circular wave, with the wave front often correlating with the smoothing cell boundaries. EGFR signaling is required for myosin accumulation and cell boundary smoothing, suggesting its propagation polarizes the planar cell rearrangement in the tracheal placode, and coordinates the timing and position of intrinsic cell internalization activities.

KEY WORDS: *Drosophila melanogaster*, EGFR, Cell intercalation, Invagination, Myosin, Trachea

INTRODUCTION

The invagination of epithelia allows the segregation of organ primordia during morphogenetic processes in development, such as gastrulation and the formation of neural tubes, gill slits and sensory organs. It involves the specification of organ placodes and the ordered internalization of epithelial sheets, followed by the epiboly-like movement of cells in neighboring regions that fill the remaining space. Apical constriction of individual cells often precedes the invagination and is thought to play important roles in gastrulation in *Drosophila* (Costa et al., 1994; Leptin and Grunewald, 1990; Oda and Tsukita, 2001; Parks and Wieschaus, 1991) and in the invagination of other organ placodes (Llimargas and Casanova, 1999; Myat and Andrew, 2000b; Simoes et al., 2006).

Cell intercalation is thought to be the major force driving the global transformation of epithelial shape, such as in embryonic body axis elongation (Irvine and Wieschaus, 1994; Keller, 2002) and gastrulation (Ettensohn, 1985; Hardin and Cheng, 1985). In *Drosophila*, the orientation of intercalating individual cells or multicellular rosettes of cells accompanies germ band extension under control of the anterior-posterior (AP) patterning system (Bertet et al., 2004; Blankenship et al., 2006; Zallen and Wieschaus, 2004). Oriented cell intercalation is also observed in elongating tracheal branches (Ribeiro et al., 2004). In addition, cell intercalation and apical constriction depend on non-muscle myosin, which is recruited to the cell-cell junctions and provides the contractile force (Bertet et al., 2004; Kiehart et al., 2000).

The tracheal system of *Drosophila* is formed by the invagination and branching of ectodermal epithelia (Manning and Krasnow, 1993; Samakovlis et al., 1996). The tracheal fate is specified at stage 10, when the HLH-PAS protein Trachealess (TRH) begins to be highly expressed in the tracheal placode (Isaac and Andrew, 1996; Wilk et al., 1996) (Fig. 1A). Apical constriction is observed in the dorsomedial region of the placode, where cells start to invaginate until all the TRH-positive cells are internalized (Fig. 1B). EGFR signaling is activated within the tracheal placode under the control of TRH (Gabay et al., 1997b). In *Egfr* mutant embryos, the prospective tracheal cells fail to concentrate F-actin at the constriction site (Brodu and Casanova, 2006), and the invagination is partially defective (Llimargas and Casanova, 1999). It is not clear, however, to what extent apical constriction and cell intercalation account for the highly coordinated process of tracheal invagination or how EGFR signaling regulates these processes. Progress in elucidating these events has been slow because of the lack of precise knowledge about the cellular movements during invagination.

Here we used time-lapse imaging to trace the dynamic movements of cells and cell interfaces before and during tracheal invagination. We show that changes in the distribution of non-muscle myosin accompanies the rearrangement of cells in the tracheal placode, which encircle the invagination site by aligning in short rows arranged in arcs (a process called 'boundary smoothing') and undergoing cell intercalation. These processes are controlled by EGFR, which is activated in an expanding circular pattern, thereby providing spatiotemporal information to cells in the tracheal placode. In the absence of EGFR, tracheal cells were internalized individually, suggesting that the key role of EGFR signaling is to coordinate the intrinsic ingression activity of the cells into the ordered process of invagination.

MATERIALS AND METHODS

Fly strains

The following fly strains were used: *sqh-GFP-Moe* (Kiehart et al., 2000), *trh-lacZ* (Kassis et al., 1992), MRLC-GFP (myosin-GFP) (Royou et al., 2004), *btl-GFP-Moe* (Kato et al., 2004), *rho-lacZ* (a gift from Drs Kenji Matsuno and Yukio Nakamura, Tokyo University of Science, Japan). Information on the following stocks can be found in FlyBase (http://flybase.net/): *rho^{del1}*, *Egfr^{f24}*, *Dsor1^{Gp158}*, *pnt^{delta88}*, *UAS-sspi*, *prd-Gal4*, *ovo^{D1} FRT101; hs-FLP^{38}*, *TM3*, *Kr-gal4 UAS-GFP*.

Imaging

Imaging was performed as previously described (Kato et al., 2004). Ten 1-μm-thick Z stacks were taken every 2 minutes over a period of up to 160 minutes. Embryos at this stage often rotated during imaging. Only images of a few successful recordings that covered the entire invagination process were

[1]Riken Center for Developmental Biology, 2-2-3 Minatojima-minamimachi, Chuo-ku Kobe 650-0047, Japan. [2]Department of biology, Kobe University Graduate School of Science, Kobe, Japan.

*Present Address: Gurdon Institute, University of Cambridge, Tennis Court Road, Cambridge CB2 1QN, UK
†Author for correspondence (e-mail: shayashi@cdb.riken.jp)

Accepted 7 September 2007

used for cell tracing. The number of successfully imaged invagination events and embryos (in parentheses) was: for GFP-Moesin-labeled embryos, control 9 (4), *rho*^{del1} 5 (2), *Egfr*^{f24} 9 (4), *pnt*^{delta88} 7 (3), and for myosin-GFP-labeled control embryos, 9 (3). Intercalating cells were marked and traced from still images, and their centroid position was determined using the measurement function of ImageJ (National Institutes of Health, USA). The angle and distance of cell displacement was calculated. The invagination site was defined as the position of the first cell to internalize. For the *Egfr*^{f24} embryos, only cases in which the invagination took place only at one position were used for analysis. The orientation of mitosis was determined in a similar manner, except that the position of invagination was defined as the centroid of the tracheal pit. Mutant embryos were identified by the absence of green balancer. Non-randomness of the orientation of cell displacement and the cell division axis were assessed by the Kolmogorov-Smirnov test.

Antibody staining

The primary antibodies were against the following proteins: DLG, E-cadherin (Developmental Studies Hybridoma Bank), anti-double phosphorylated ERK (dp-ERK; Sigma), KNI (Kosman et al., 1998), GFP (rabbit, MBL; chick, Chemicon), myosin heavy chain (MHC: a gift from Fumio Matsuzaki, RIKEN, Center for Developmental Biology, Kobe, Japan) and β-galactosidase (Cappel). The dp-ERK signal was amplified with a TSA indirect kit (Perkin Elmer Life Sciences). Signal intensity of MHC-stained cell boundaries were quantified by the use of ImageJ and the statistical significance was tested by Student's *t*-test (two-sample assuming equal variances, two-tail).

RESULTS

Tracheal invagination proceeds in morphologically distinct phases

To study the shape changes, movement, and proliferation of tracheal primordial cells, we used time-lapse imaging to observe embryos labeled with the F-actin marker GFP-Moesin (Kiehart et al., 2000) or myosin marker MRLC-GFP (Royou et al., 2004) (hereafter called myosin-GFP; Fig. 2, control, see Movies 1, 2 in the supplementary material) and compared the results with the images of fixed preparations (Fig. 1A,B) (Brodu and Casanova, 2006; Isaac and Andrew, 1996; Llimargas and Casanova, 1999; Manning and Krasnow, 1993; Wilk et al., 1996). The use of GFP markers allowed us to compare the dynamic distribution of F-actin and myosin during invagination.

About 50-70 minutes prior to the start of invagination, at cycle 15 of embryogenesis, the dorsal ectodermal cells entered mitotic quiescence (Fig. 2A and see Movie 1 in the supplementary material). Then, about 10 cells in the dorsal-medial part of the placode started to show apical constriction (Fig. 1Ba; Fig. 2B, yellow; defined as a reduction of apical cell surface below 5 μm^2) and shifted basally about 3 μm (Fig. 1Bb, defined as time 0'). The cells with the constricted apical surfaces then became internalized, leaving a cleft called the tracheal pit (Fig. 1Bc, Fig. 2B, pink). Subsequently, cell internalization continued without apparent apical constriction (Fig. 1Bd), and mitotic activities resumed around the tracheal pit (Fig. 1Bc,d, Fig. 2B, asterisks). Time course analyses of apical constriction showed that those cells that internalized with sharply constricted apices (<1 μm^2) were clustered at the center of the placode (Fig. 1C, red outline). We also mapped the timing of cell internalization within the tracheal placode and found that cells that internalize early were clustered at the center, surrounded by later internalizing cells in a stepwise manner, forming concentric circles (Fig. 1C). The cell size and temporal analyses of cell internalization demonstrated that the cells around a prospective tracheal pit internalized first with apical constriction (phase 1), followed by those surrounding them, with less extensive apical constriction (Fig. 1C). The timetable of the tracheal invagination events is shown in Fig. 1E.

Oriented cell intercalation and cell division in the tracheal placode

To examine how the concentric groups of cells formed, we analyzed the pattern of cell intercalation in the 30-minute period prior to invagination, by tracing the relative positions of neighboring cells (Fig. 3A, blue and red arrows). The direction of cell displacement was quantified by measuring the angle of the line connecting the centroids of the two displaced cells (Fig. 3B). We tested two alternative hypotheses, (1) that cell intercalation follows a polar coordinate system with the center situated at the point of invagination, or (2) that it follows a Cartesian coordinate system defined by the AP and DV (dorsal-ventral) embryonic axes. The displacement angle relative to the polar coordinate ($|\theta|$) was 24.4±3.4° [average and standard error (s.e.m.), n=21]. This value greatly deviates from the average of 45° that would be expected if displacement occurred randomly (Kolmogorov-Smirnov test, $P<0.05$). However, the average angle relative to the AP axis ($|\theta'|$) was 41.8±6.1° (n=18), which was judged to be random. Therefore, the result favors the polar coordinate model.

After the initiation of invagination, the tracheal cells entered a final wave of mitosis. The orientation of the cell-division axis of the placodal cells was significantly biased toward the center of the tracheal pit ($|\theta|$=14.6±2.78°, n=22, $P<0.01$; Fig. 1D). A radial orientation of cell division might help direct cells to flow into the site of invagination. Taken together, these observations indicate that the orientation of the cell displacement prior to invagination (phase 1), and the cell division axis in phase 2 of invagination in the tracheal placode are both aligned toward the site of invagination, suggesting that the planar cell polarity in the tracheal placode is polarized toward the invagination site.

Cell-boundary smoothing correlates with transient myosin accumulation

In the neighborhood of the tracheal placode cells undergoing intercalation and we frequently noted groups of four to six cells forming arc-like rows that collectively surrounded the future invagination site (Fig. 3A, time 2'). By tracing the contours of the cells in these rows, we found that these smooth arcs of well-aligned cells arose from rows of cells whose contours formed zig-zagging boundaries (Fig. 3A; green and orange lines). We call this process 'cell-boundary smoothing' and characterized its cellular properties by monitoring the accumulation pattern of myosin-GFP (Royou et al., 2002) as a marker for contractility of the cell-cell junctions (Bertet et al., 2004; Kiehart et al., 2000) (see Fig. 6 for quantitative assessment of this process). Myosin-GFP was highly concentrated at the dorsal border of the ectoderm that had begun to form the contractile supracellular actomyosin purse string (Kiehart et al., 2000) (Fig. 3C), suggesting that myosin-GFP accumulation is a hallmark of contractile activity at cell junctions. When dorsal ectodermal cells entered mitotic quiescence before invagination, the myosin-GFP level in apical cell interface was generally low except for a high accumulation between the straight rows of cells abutting the segment boundary (see Movie 2 in the supplementary material, time –40'). The prominent dot-like signals in each cell appeared to be an artifact of the GFP fusion protein, because they were not detected with anti-myosin heavy chain (MHC) antibody staining (Fig. 6B) and were not considered further. In the next 20 minutes, myosin-GFP accumulated at the apical cell junctions of other ectodermal cells in non-uniform and rapidly changing patterns. The signal was especially upregulated in shrinking cell junctions undergoing cell intercalation (Fig. 3E) (Bertet et al., 2004). When the arc-like rows of cells started to appear in the tracheal placode,

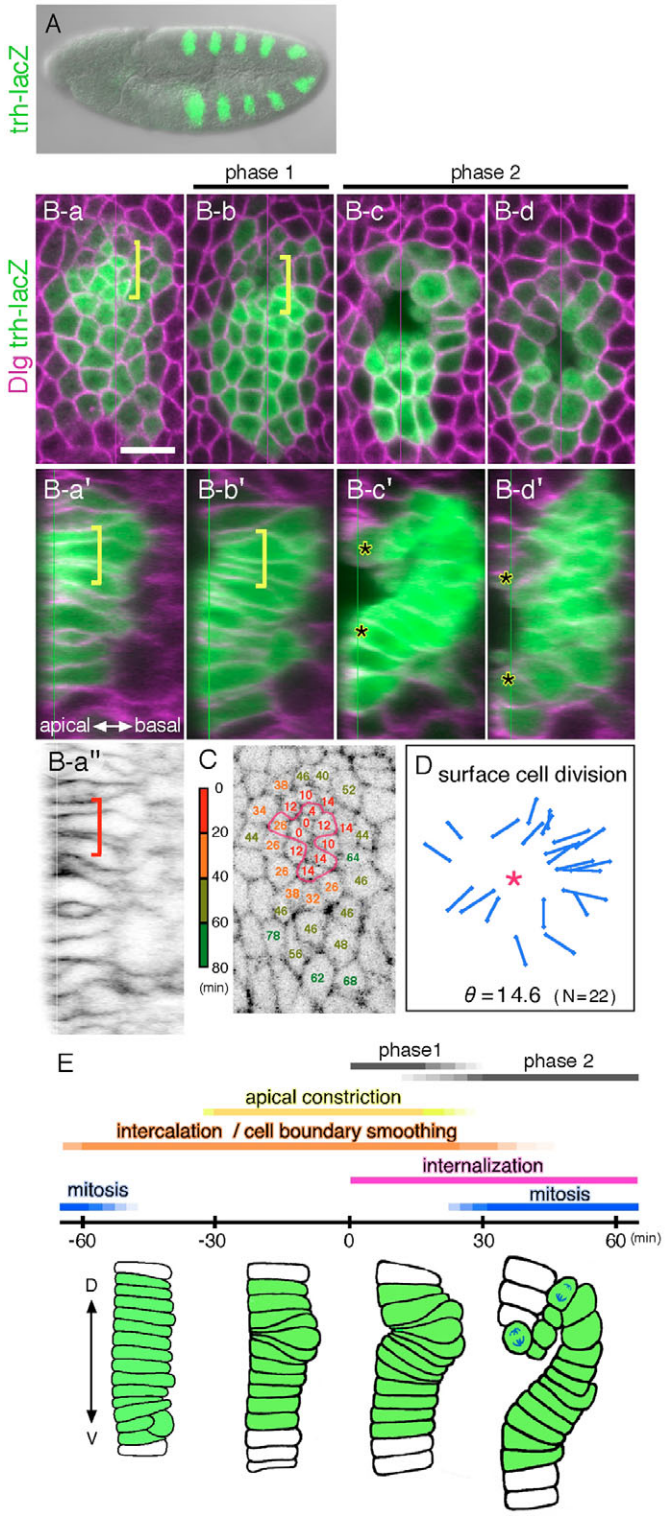

Fig. 1. Overview of tracheal invagination. (**A**) A stage 10 embryo expressing *trh-lacZ* (green). (**B**) Cell shape changes in the tracheal placode in four successive stages of invagination. *x-y* (Ba-Bd) and *y-z* (Ba'-Bd') confocal sections of fixed embryos expressing *trh-lacZ* (green) and DLG (Dlg; magenta) are shown. The bracket indicates internalizing cells with apical constriction (phase 1). Asterisks indicate internalizing cells without apical constriction (phase 2). The thin red and green lines indicate the position where the confocal sections were made. Ba" is a gray-scale image of the DLG signal. (**C**) Spatiotemporal order of the cell internalization events in a control *sqh-GFP-Moe* embryo. Tracheal placode cells at time –48 minutes are labeled with a number indicating their time of internalization, which was measured by tracing individual cells in time-lapse movie (see Movie 1 in the supplementary material). The cells internalized with a constricted cell apex (<1 μm^2) are marked by a red line. (**D**) The orientation of cell divisions in the tracheal placode of a control *sqh-GFP-Moe* embryo after the onset of invagination. The asterisk at the center indicates the invagination site. (**E**) Summary of the time course of apical constriction, cell intercalation and internalization, and mitosis in the tracheal placode. The time when the first cell disappeared from the apical plane of the tracheal placode was set as time 0. Scale bar: 10 μm.

the myosin-GFP accumulation was often elevated in the smoothed boundaries of the cellular arcs surrounding the invagination site (Fig. 3C and see Movie 2 in the supplementary material). We also noted a number of cell intercalation events associated with smoothing boundaries (Fig. 3A).

The enrichment of myosin-GFP in the arc-like row boundaries was transient, and took place in multiple waves: first in cells that invaginated early, and then in later-invaginating cells (Fig. 3D, boundary sets indicated with blue, green, and magenta lines; see Movie 2 in the supplementary material). Tracing the time-lapse images revealed that these arc-like boundaries were formed as initially separate cells, or ones that were newly juxtaposed, aligned themselves into continuous rows (Fig. 3D). Thus, the formation of a smooth row contour from an initially discontinuous and zig-zagging row boundary was accompanied by an elevated accumulation of myosin-GFP. As the rows of cells moved closer to the invagination site, their boundaries became discontinuous again (see the boundary marked in blue, Fig. 3D, time –2'). Therefore, the observed boundary smoothing was transient. Increase in myosin-GFP along cell boundaries was also detected in other parts of the ectoderm, but it appeared to be random and did not correlate with cell movement. For example, the tracing of cell contours in the dorsal ectoderm revealed that although these boundaries were occasionally broken by the insertion of new cells, their positions and mutual relationship remained relatively constant (Fig. 3D, orange lines). These dynamic patterns of myosin-GFP accumulation were different from the distribution of F-actin revealed by GFP-Moesin (Fig. 3A), which was more uniform and constant, suggesting that the selective recruitment of myosin to cell junctions might trigger localized contractile activities. We concluded that many cells in the tracheal placode are rearranged into transient arc-like rows through the processes of cell intercalation and smoothing of arc-like cell boundaries.

Spatial and temporal changes in ERK activation during invagination

As a candidate signal for coordinating the boundary smoothing and cell intercalation, we studied the expression pattern of EGFR signaling. Active ERK MAP kinase was visualized with an anti-double phosphorylated ERK (dp-ERK) antibody (Gabay et al., 1997a). dp-ERK was first detected in both the cytoplasm and nuclei of the cells in the tracheal placode before they entered mitotic quiescence and started to constrict apices (Fig. 4A), in a pattern roughly overlapping with the expression of the EGFR activator *rhomboid* (*rho*; Fig. 4F; detected by the expression of *rho-lacZ*),

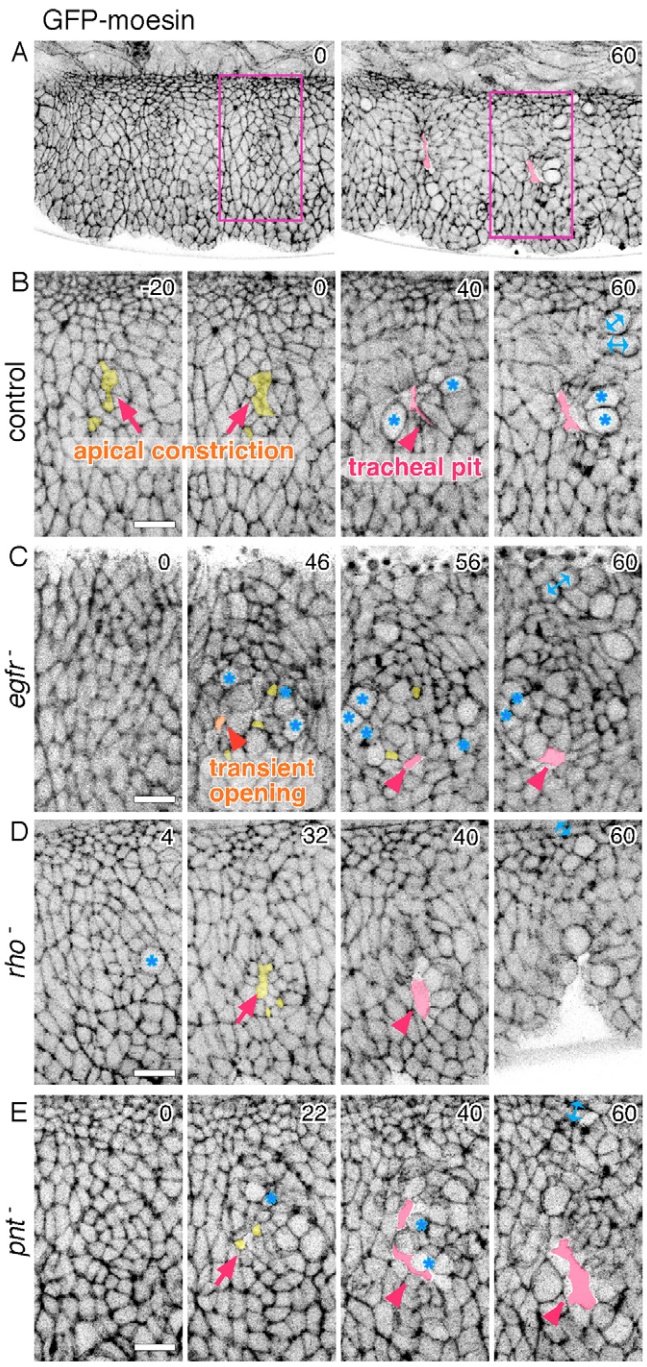

Fig. 2. Time-lapse analysis of tracheal invagination. Cell boundaries were labeled with GFP-Moesin. The number in the top-right corner is the elapsed time in minutes. In a control embryo (**A**,**B**, and see Movie 1 in the supplementary material), time 0 was defined as the start of invagination. Cell division in the dorsal ectoderm outside of the tracheal placode resumed at about 60 minutes (blue double-headed arrow). For mutant embryos, the time of dorsal cell division was defined as 60 minutes. Apically constricted cells (<5 μm^2) are colored yellow and the tracheal pit (the space emptied by the internalized cells) is colored pink. Mitotic cells in the tracheal placode are marked with blue asterisks. The region corresponding to the magenta rectangle in A is enlarged in B. In mutant embryos of *Egfr* (**C**; see Movie 3 in the supplementary material), *rho* (**D**; see Movie 4 in the supplementary material) and *pnt* (**E**; see Movie 5 in the supplementary material), the apical constriction was lost or reduced, the onset of invagination was delayed, and precocious mitosis was observed. In *Egfr* mutants (C), transient pit-like openings (colored orange) due to the ingression of one to two cells were observed multiple times (six times in this example, see Movie 4 in the supplementary material). Scale bars: 10 μm.

within the cells in the tracheal placode expressing *trh-lacZ* and KNI (Fig. 4F,G). The dp-ERK expression then expanded to cover the dorsal half of the placode (Fig. 4B). A *y-z* sectional view of the tracheal placode doubly labeled for dp-ERK and nuclei (Fig. 4Bb) showed that the dp-ERK in the central domain was concentrated in the apical cell cortex, and in the peripheral domain it accumulated in both the cytoplasm and nuclei. Thus, cells with nuclear dp-ERK signals formed a ring in a horizontal optical section at the basolateral level (Fig. 4Bc). We found no sign of apical constriction and cell boundary smoothing was partial at this stage (Fig. 4Bd,e). During the next stage, cell boundary smoothing proceeded and the central cells with an apical accumulation of dp-ERK showed constricted apices and invaginated, and then rapidly lost the dp-ERK signal during phase 2 of invagination, when mitotic activity resumed (Fig. 4C and see Fig. S1 in the supplementary material). dp-ERK was reduced in *rho* mutants (data not shown), and lost completely in *Egfr* mutants (Fig. 4D,E). We concluded that the intracellular location of the dp-ERK changed from nuclear and cytoplasmic to the apical cortex in about a 30-minute period prior to invagination, and dp-ERK was subsequently eliminated after the onset of invagination. In the tracheal placode, the pattern of nuclear dp-ERK expression was spatiotemporally regulated by EGFR: it originated from a central spot and expanded into a ring that encircled the prospective site of the apical constriction and invagination.

EGFR signaling is required for apical constriction and proper timing of tracheal invagination

EGFR signaling is required for tracheal cell invagination (Llimargas and Casanova, 1999; Wappner et al., 1997). In mutants of *rho*, a positive regulator of EGFR signaling, some tracheal precursor cells fail to invaginate and remain at the epithelial surface (Llimargas and Casanova, 1999) (Fig. 5B). A similar phenotype is observed in mutants of EGFR and the ETS domain transcription factor Pointed (PNT), a key target of ERK signaling (Brunner et al., 1994; O'Neill et al., 1994) (Fig. 5C,D), suggesting that EGFR signaling and its nuclear transduction are essential for proper invagination.

To investigate the role of EGFR signaling in the tracheal placode invagination events, time-lapse imaging of *rho*, *Egfr* and *pnt* mutants was performed, and their phenotypes were compared with that of control embryos. As a staging reference, we used the cell division in the dorsal epidermis that normally resumes about 60 minutes after the onset of invagination (Fig. 2B-E). We found that defects in the *Egfr* mutants were already apparent at the onset of invagination. In the *Egfr* mutants apical constriction was nearly absent (Fig. 2C, compared with the yellow-colored cells in 2B), and the remaining apical constriction event did not correlate with the position of invagination. These defects in apical constriction are consistent with a previous report implicating EGFR signaling in the initiation of local F-actin assembly (Brodu and Casanova, 2006). Furthermore, we found that the onset of invagination was delayed in the *Egfr* mutants, and some cells resumed mitosis before the start of invagination (Fig. 2C, 46 minutes, asterisk), suggesting that the

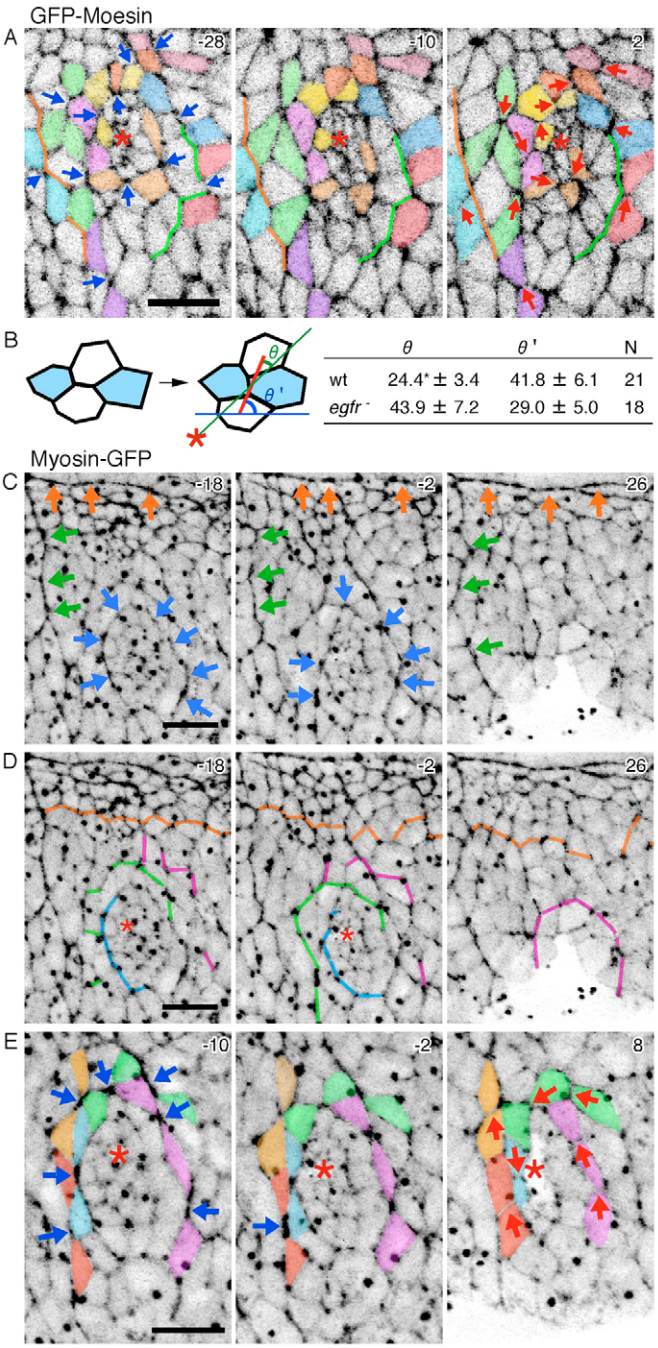

Fig. 3. Cell-row boundary smoothing and cell intercalation prior to invagination. See Movies 1 and 2 in the supplementary material. (**A**) GFP-Moesin. Intercalating cells are shown in the same color. Shrinking cell boundaries and newly formed cell boundaries are indicated by blue and red arrows, respectively. The position of the tracheal pit is indicated by a red asterisk. Examples of cellular arc formation are indicated by orange and green lines. (**B**) Analyses of the cell displacement angle. Mean±s.e.m. are shown. Asterisk indicates significant (P<0.05) deviation from random orientation (average 45°). See text for details. (**C-E**) Transient accumulation of myosin-GFP at the cell-cell interface. (C) Continuous rows of myosin-GFP-enriched cell-row boundaries are indicated by arrows. Cell boundaries at the segment border and dorsal ectodermal margin (green and orange arrows, respectively) stably accumulated myosin-GFP. Myosin-GFP accumulation in the arc-like cell-row boundaries surrounding the invagination site was transient and appeared as temporary waves (blue arrows, see also Movie 2 in the supplementary material). (D) Cell boundary tracing. Each arc-like boundary was formed by the joining of zig-zagging and discontinuous boundaries, which changed with the arrangement of the cells relative to one another (blue, green and magenta lines). The boundary marked with blue lines became discontinuous before entering the tracheal pit. The orange lines indicate cell boundaries in dorsal ectoderm, which were more stable. Red asterisk indicates the invagination site. (E) High accumulation of myosin-GFP in shrinking cell boundaries. For explanation of colored areas, see A. Scale bars: 10 μm.

temporal order of invagination and mitosis was miscoordinated. The delayed invagination was confirmed by examining fixed mutant embryos. In control embryos, tracheal precursor cells started to constrict their apices and shift basally when the groove between the maxilla and labium ingressed deeply, but no such morphological changes were detected in the tracheal placodes of *Egfr* mutants at the equivalent stage (data not shown). We also imaged *rho* and *pnt* mutant embryos and found that invagination was delayed and apical constriction was less extensive than in control embryos (Fig. 2D,E and see Movies 4, 5 in the supplementary material). In addition, we monitored cell boundaries in *pnt* mutants and found some degree of smoothing (see Fig. S2 in the supplementary material). The phenotypes of *rho* and *pnt* mutants are weaker version of the *Egfr* mutant phenotype. These data suggest that EGFR signaling is required for the apical constriction and specification of the timing of invagination.

EGFR mutants are defective in cell rearrangement and restriction of the invagination site to a single focus

We next assessed the position of the tracheal pits in control and mutant embryos. In the control embryos, a single tracheal pit opened at the dorsal part of the tracheal placode (at about 25% of the length of the tracheal placode from the dorsal margin; Fig. 5H). In *Egfr* mutants, the tracheal placode expanded ventrally to include more cells at the expense of reduced ventral ectoderm (Fig. 5F) (Raz and Shilo, 1993). In the expanded tracheal placode of the *Egfr* mutants, the position of the tracheal pit was more variable and tended to shift ventrally, and occasionally two tracheal pit-like indentations were observed (Fig. 5G,I). To determine whether ERK signaling was involved in this process, we studied the phenotype of maternal-zygotic mutants of *Dsor1*, which completely lack ERK kinase activity (Hou et al., 1995; Tsuda et al., 1993). These mutants had misplaced and duplicated tracheal pits (Fig. 5J). Time course analyses of the *Egfr* mutants revealed multiple incidences of one or two cells being internalized prior to the full invagination of the larger group of cells forming the visible tracheal pit (Fig. 2C and see Movie 3 in the supplementary material). Most of the cells undergoing these individual internalization events were adjacent to mitotic cells.

Although frequent mitosis appeared to interrupt the cell rearrangement process, we were able to detect some arc-like cellular rows in the *Egfr* mutant placode (Fig. 2C, time 60'; see Movie 3 in the supplementary material). However, the pattern of these arc-like rows did not correlate with the position of the invagination site (Fig. 2C). We also detected a limited number of cell intercalation events, and measurement of their orientation revealed a |θ| that was judged

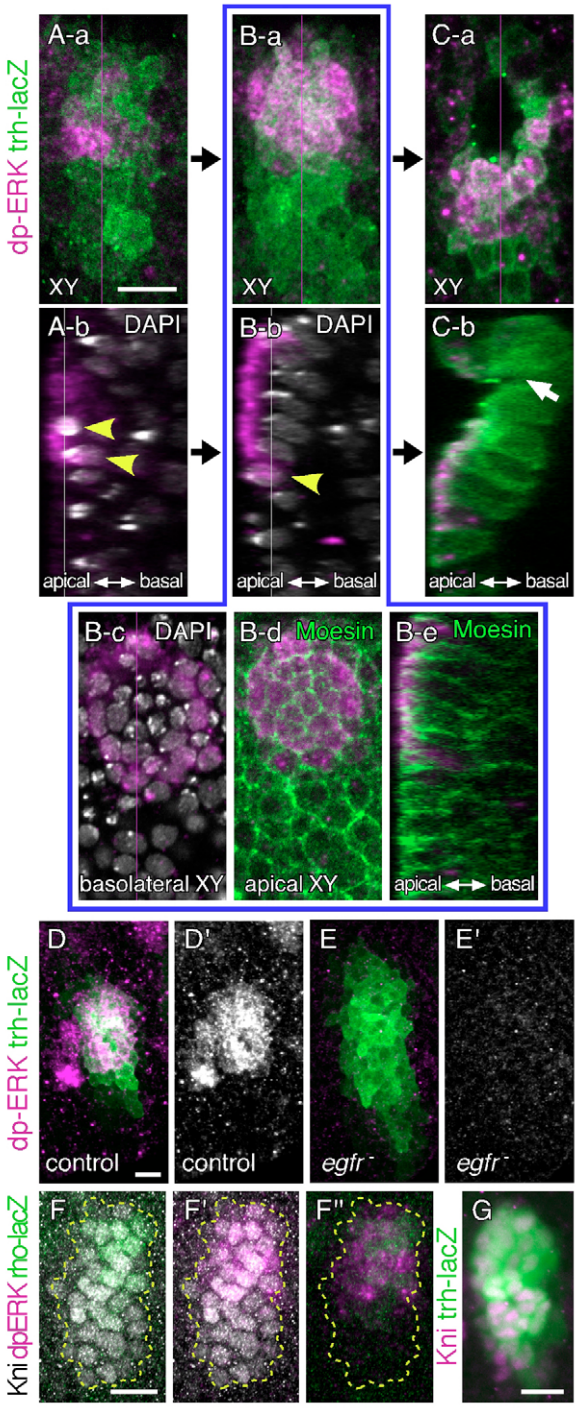

Fig. 4. The dynamic pattern of EGFR activity detected with dp-ERK. (**A-C**) Spatiotemporal patterns of dp-ERK in three successive stages of invagination. Cells were labeled for dp-ERK (magenta), *trh-lacZ* (green), GFP-Moesin (green) expression; DNA is shown in gray scale; *x-y* and *y-z* sections of the same placode (labeled with a and b, respectively) are shown for each time point. Additional views of B are shown in Bc to Be. dp-ERK expression was initially detected in the nucleus and the cytoplasm of a few cells in the dorsal side of the tracheal placode (A, arrowhead) and subsequently expanded to fill the entire dorsal half of the placode (B). dp-ERK showed a nuclear localization in the peripheral region (arrowhead) and was concentrated in the apical cytoplasm in the central region. Note that Bc is a deeper optical section of Ba and Bd (position of the section is indicated by a thin white line in Bb). Apical constriction had not yet occurred and only a mild degree of cell boundary smoothing was observed at this stage (Bd). The dp-ERK signal was downregulated after invagination (C). (**D**,**E**) dp-ERK expression in $Egfr^{+/-}$ (D) and $Egfr^{-/-}$ (E) embryos. D′,E′ show the dp-ERK signal. (**F**) *rho-lacZ* expression was very similar to the pattern of dp-ERK. The tracheal placode (dashed outline) was marked with KNI (Kni). (**G**) The overlap of KNI and *trh-lacZ* expression. Scale bars: 10 μm.

to be non-biased (43.9±7.2°, $P>0.05$). Taken together, these results suggest that EGFR signaling is required for the proper patterning of cell rearrangement and to restrict the site of tracheal invagination to a single focus at the dorsal region in tracheal primordia.

Regulation of cortical myosin recruitment by EGFR signaling

We next investigated the role of EGFR signaling in the regulation of myosin recruitment to cell-row boundaries. We found that the outer boundaries of cells with high nuclear dp-ERK often correlated with the arcs of cells with a high accumulation of myosin-GFP (Fig. 6Aa and see Fig. S1 in the supplementary material). To determine whether EGFR was required for this myosin accumulation, we stained embryos with an antibody against MHC. The staining revealed the smoothed boundaries of cells aligned in arc-like rows in the tracheal placode of control embryos (Fig. 6B). In order to quantify the occurrence of arc-like rows, we classified tricellular junctions in the tracheal placode into two classes (Fig. 6D). Class T junctions contain two of the cell interfaces forming an angle of 180±30°. Other junctions were classified as class Y. Cells were judged to be forming an arc if 'horizontal' class T junctions (Fig. 6D) were found in adjacent cells (less than one cell boundary apart). In control tracheal placodes (*Egfr*/+, $n=3$), an average of 11.0 class T junctions were observed per placode (T+Y=83 per placode), and 7.3 (66%) of them were judged to be in arcs. No such arc-like rows were apparent in *Egfr* mutants (Fig. 6C). The average number of class T junctions was reduced to 5.2 per placode despite 49% increase in placode size (T+Y=124 per placode). We found one case where three class T junctions were in a row. It is likely that those cells were not participating in invagination (Fig. 2C and see Movie 3 in the supplementary material).

To quantify the differential distribution of myosin, we classified cell boundaries of class T junctions into horizontal and vertical (Fig. 6D), and their intensity was compared. Intensity of horizontal class T boundaries was 1.52±0.11(mean±s.e.m., arbitrary unit, $n=33$), that was significantly increased compared to 1.00±0.11 in vertical boundaries ($n=37$, $P<0.002$, Student's t-test). Such enrichment of myosin to horizontal boundaries was observed in class T junctions both in arcs or not. Since two-thirds of class T junctions formed arcs, we conclude that myosin is preferentially enriched in cell junctions consisting of arcs.

To test whether EGFR was capable of inducing this cortical myosin accumulation, we ectopically activated EGFR in otherwise flat epithelia by expressing the secreted (activated) form of an EGFR ligand, Spitz (sSPI) (Schweitzer et al., 1995). The expression of sSPI by the paired enhancer (Brand and Perrimon, 1993) activated ERK kinase in broad bands that covered the even-numbered parasegments. At the interface of cells expressing ectopic dp-ERK

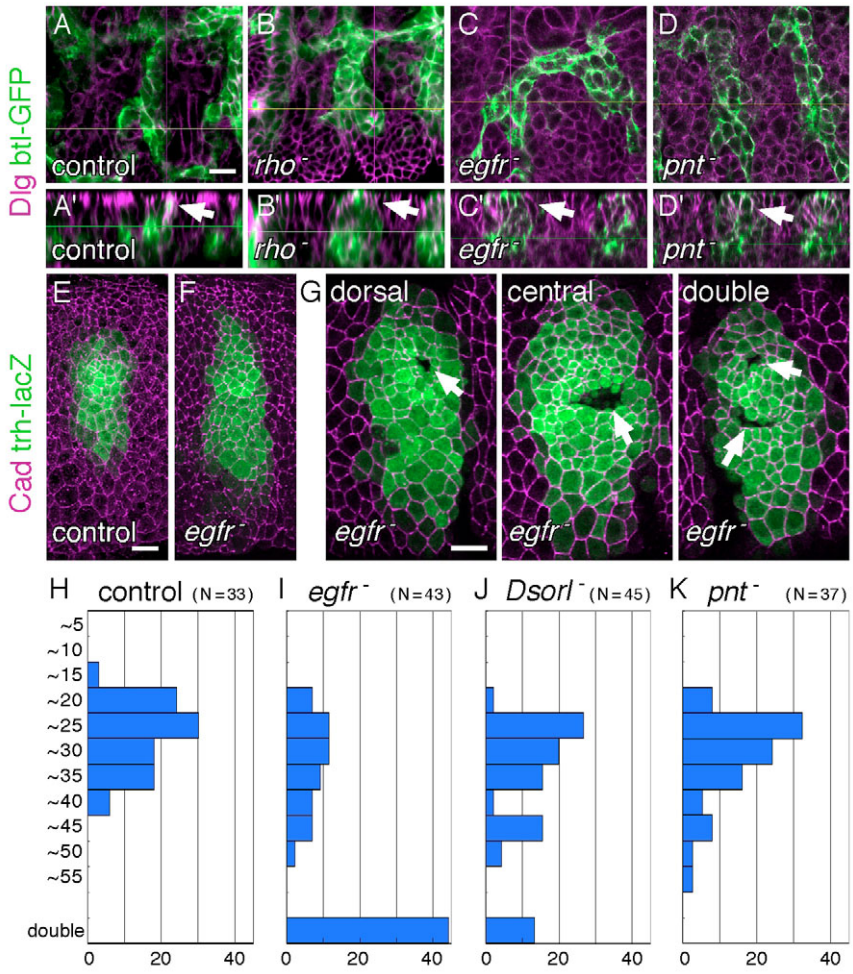

Fig. 5. Invagination defects in EGFR-related mutants. Tracheal invagination phenotypes in stage 14 embryos. (**A**) All of the *btl-GFP*-expressing cells were internal except for the spiracle cells (arrow). (**B-D**) Many of the *btl-GFP*-expressing cells remained external in the *rho* (B), *Egfr* (C), and *pnt* (D) mutants. (**E**,**F**) The tracheal placode expanded ~1.5 fold in the $Egfr^{-/-}$ (F) compared with $Egf^{+/-}$ (E) embryos. (**G**) In the *Egfr* mutants, the invagination position (arrows) was variable and sometimes duplicated. (**H-K**) Position of invagination sites (% position measured from the dorsal edge) and the number of sites in controls, and in *Egfr*, *Dsor1* and *pnt* mutants. The incidence of double invagination observed in *Egfr* and *Dsor1* embryos was counted separately, without reference to their position. Scale bars: 10 μm.

and their neighbors, we often observed an elevated myosin accumulation (Fig. 6E, arrowheads). Comparison of myosin accumulation in this type of border (DV borders, Fig. 6F) versus intersecting borders (AP borders) demonstrated that dp-ERK activation specifically enriched myosin accumulation in the interface with low dp-ERK-expressing cells (Fig. 6F). The result suggests that the juxtaposition of cells with high and low levels of EGFR activity can trigger myosin accumulation at the cell interface. Furthermore, within the region of high dp-ERK activity, we noted the formation of deep epidermal depressions at the sites where segmental furrows would form (Fig. 6E, asterisk): the depressed region had abundant cells with constricted apices and became continuous with the expanded tracheal pit. The odd-numbered parasegments remained flat (arrow). These results suggest that a high level of EGFR signaling promotes the apical constriction of epidermal cells and precocious epidermal depression.

DISCUSSION

The mechanical basis of invagination has long been a subject of debate. Cell-shape change, cell migration and cell intercalation are some of the proposed mechanisms (reviewed by Keller et al., 2003). Apical constriction converts cells into a bottle-like shape and is thought to be an important process in invagination (Myat and Andrew, 2000a). However, the observation that cells can be internalized without undergoing apical constriction during normal invagination of the *Drosophila* mesoderm (Oda and Tsukita, 2001) and trachea (this work), and as a result of mutations that disturb apical constriction but allow the invagination of a majority of placodal cells (Llimargas and Casanova, 1999; Oda and Tsukita, 2001; Sweeton et al., 1991) suggest that the critical role of apical constriction is not in invagination per se, but is likely to be modulatory. We have shown here that invagination of the tracheal placode involves, prior to the start of invagination, the rearrangement of cells to form multicellular arcs with smooth boundaries. We have also shown here that polarized cell intercalation and boundary smoothing take place simultaneously in multiple waves, and together with apical constriction, coordinate the cells' intrinsic internalization activities to allow precisely regulated invagination. Our findings suggest a model in which EGFR signaling regulates this process (Fig. 6G).

The role of localized myosin activity in invagination

We have shown that the accumulation of myosin-GFP was elevated in the boundaries of cells that were arranged in arc-like rows. The linkage of a cortical actomyosin network through such a chain of cells via a cell-cell adhesion complex would result in the formation of supracellular actomyosin cables similar to those observed at the leading edge of the dorsal epidermis (Hutson et al., 2003; Kiehart et al., 2000). Although the cables formed were transient and weak compared with their counterparts in the epidermal leading edge, their contractile force in convex cell contours would help smooth the boundary and compress cells toward the center, thereby accounting, at least in part, for the dense cell packing in the prospective tracheal

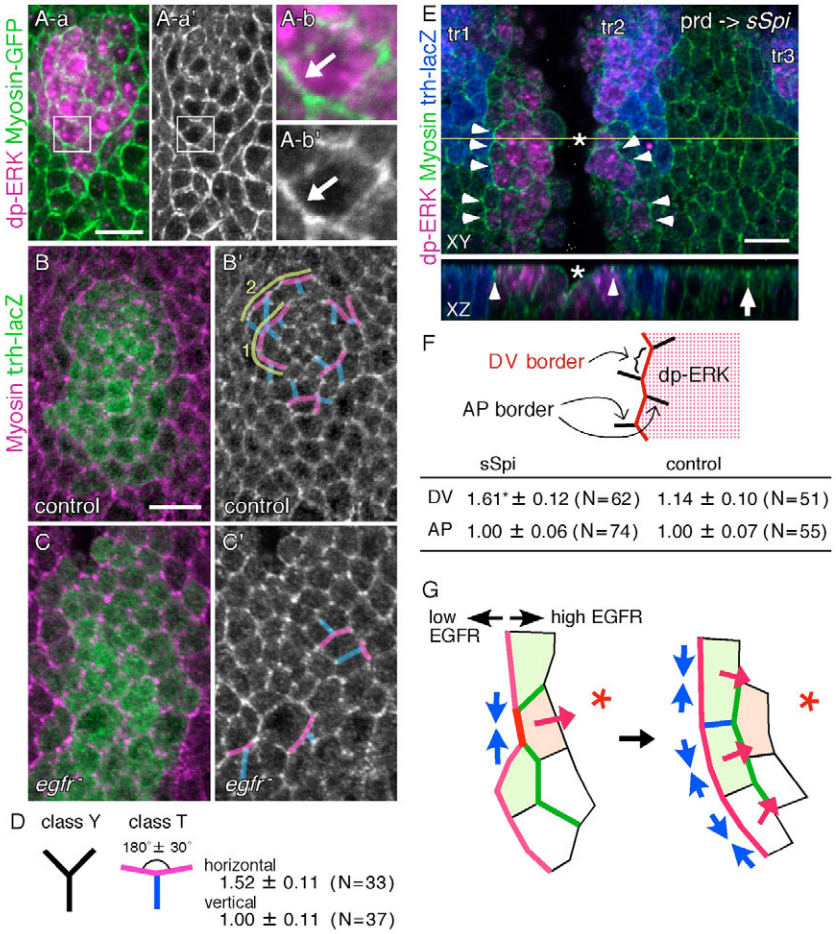

Fig. 6. EGFR regulates cortical myosin accumulation. (**A**) Cell boundaries with high myosin-GFP accumulation often corresponded to the outer boundary of dp-ERK. b and b′ are higher magnification images of a and a′, respectively. Arrows indicate the high myosin-GFP accumulation at the interface of cells with high and low dp-ERK levels. (**B**,**C**) MHC accumulated in arc-like patterns in *Egfr* heterozygous embryos, but these patterns were lost in *Egfr* homozygotes (see text for quantitative assessment). In B′, 8 out of 12 class T junctions were judged to be in arcs. Two examples of arcs are highlighted with yellow curved lines 1 and 2. (**D**) Two classes of tricellular junctions. In class T junctions, 'horizontal' cell boundaries are colored pink, and 'vertical' ones, blue. Myosin concentration was more than 50% enriched in horizontal cell junctions compared to the vertical one (mean±s.e.m., arbitrary unit, number of measurement indicated in parentheses, $P<0.002$, Student's *t*-test). (**E**) Expression of sSPI (sSpi) by the *prd* enhancer in even-numbered parasegments induced the massive activation of ERK and accumulation of MHC at the cell boundaries between cells with high and low dp-ERK expression (arrowheads). sSPI also induced the precocious invagination of the segmental furrow (asterisk) that becomes contiguous with the tracheal pit (tr2). An arrow indicates unaffected segment boundary. (**F**) Enrichment of junctional myosin by sSPI. The intensity of myosin signal was compared between the border along the stripe of elevated dp-ERK (DV border, red lines) and those intersecting them (AP border, black lines; mean±s.e.m., arbitrary unit). sSpi significantly increased the DV boundary signal compared to AP boundary (*, $P<10^{-5}$, Student's *t*-test: two-sample assuming equal variances, two-tail). No such enrichment was observed in the control segments. (**G**) A model for the EGFR-dependent coordination of cell movement. Left: Myosin accumulates at the boundary of cells with high and low EGFR activity. The contractile force of myosin (blue arrows) helps shrinkage of cell boundary and cell intercalation (juxtaposed cell boundaries shown in green). In addition, the contractile force smoothens other cell-row boundaries. Right: once the cell-row boundaries form a continuous arc, the net force in the convex contractile supracellular actomyosin cable (pink) is oriented toward the inside of the arc (magenta arrows). Red asterisk indicates the invagination site. Scale bars: 10 μm.

pit. In addition, polarized cell intercalation contributes to cell packing by pushing cells toward the center and connecting cell boundaries to form larger arcs. These packed, apically constricted cells were first to internalize (Fig. 6G).

Coordination of cell rearrangement by a wave of EGFR signaling

Although it was previously noted that EGFR plays an important role in the accumulation of myosin in cells undergoing apical constriction (Brodu and Casanova, 2006), it was not clear whether EGFR influences cells surrounding the invagination site. Here we showed that the nuclear transduction of EGFR signaling monitored by dp-ERK formed a transient wave that swept from the center to the periphery of the placode. Since PNT, the major nuclear target of EGFR-ERK signaling, was required in this process, nuclear dp-ERK must represent the major EGFR signaling output required for invagination. Our observation that nuclear dp-ERK was already extinguished at the time of invagination suggests that the effect of EGFR in invagination might be indirect. Since the spreading front of the dp-ERK often correlated with high myosin accumulation, we speculate that the circular propagation of EGFR signaling in the peripheral region helps to specify the cell-cell interface where myosin accumulates.

A good candidate for the link between nuclear dp-ERK and myosin regulation is the RHO GAP gene *cv-c*, which is transcriptionally upregulated by EGFR (Brodu and Casanova, 2006). Since RHO GAP is linked to the regulation of myosin contractility through the RHO-RHO kinase-myosin regulatory light-chain pathway (Amano et al., 1997; Winter et al., 2001), the transcriptional activation of *cv-c* within a region of high EGFR activity should downregulate myosin activity. Although the mechanism is not known, a difference in myosin activity between neighboring cells might trigger contractile activity. It follows that the circular spread of EGFR activity would cause the sequential modulation of myosin contractility throughout the tracheal placode. The requirement for *pnt* for proper invagination indicates transcriptional regulation is essential. However, the relatively weaker invagination phenotype in *pnt* mutants compared to *Egfr* mutants suggests that another nuclear target, or a non-nuclear pathway of EGFR signaling through apically accumulated dp-ERK regulates invagination.

In *Egfr* mutants, the onset of invagination was delayed and took place at variable positions, and phase 1 of invagination was apparently skipped. These phenotypes can be explained by the loss of the putative centripetal force driven by the myosin-dependent contraction of the arc-like rows of cells. One striking observation in

the *Egfr* mutants was the internalization of multiple individual cells prior to invagination. This observation indicates that EGFR is dispensable for cell internalization per se, but is essential for focusing the cell internalization activity, thus specifying the time and place of the initial invagination. This result also indicates that cells in the tracheal placode possess an EGFR-independent cell-ingression activity. Although the origin of this activity is not understood, it may be under the control of genes specifying the tracheal placode, such as *trh* and *vvl*. It is interesting to note that the cell internalization events observed in the *Egfr* mutants were often associated with mitosis, which might alter the local surface tension in the placode to permit neighboring cells to ingress. Thus, EGFR seems to restrict the invagination site to one place through two mechanisms: first by coordinating the circular cell rearrangement, and second by suppressing cell division to stabilize the surface tension of the placode.

The activation of EGFR signaling started from one spot and spread out in a ring that encircled the prospective invagination site. Since the pattern of *rho* transcription was not sharply focused in the tracheal placode, it is likely that the secreted Spitz ligand is broadly distributed. The circular spread of EGFR activation from this crude distribution of EGFR ligand might require feedback regulation of EGFR signaling (Shilo, 2005), as has been shown in other cases (Brodu et al., 2004; Wasserman and Freeman, 1998).

In this study, the precise mapping of dp-ERK and cell behaviors allowed us to demonstrate the role of EGFR signaling in cell rearrangement. *Drosophila* leg development bears several similarities to tracheal invagination: it develops by evagination, a process fundamentally similar to invagination, and requires graded EGFR activity (Campbell, 2002; Galindo et al., 2002) and TRH (Tajiri et al., 2006). FGF signaling is known to have a role in the invagination of the lens and otic placode in the chick and mouse (Faber et al., 2001; Ladher et al., 2005). The concept of cell rearrangement at the signal propagation front may be useful for understanding the cellular mechanisms underlying the shape transformation of other organ placodes under the control of receptor tyrosine kinases.

We are grateful to Kagayaki Kato (RIKEN, CDB) for help with the image analysis. We thank Jordi Cassanova, Dan Kiehart, Fumio Matsuzaki, Kenji Matsuno, Yukio Nakamura, the Bloomington Stock Center and the Developmental Study Hybridoma Bank, for *Drosophila* strains and antibodies, and members of the Hayashi laboratory for helpful comments on the manuscript. This work was supported by a Grant-in-Aid for Scientific Research on Priority Areas (C) 'Genome Science' from MEXT Japan.

Supplementary material

Supplementary material for this article is available at
http://dev.biologists.org/cgi/content/full/134/23/4273/DC1

References

Amano, M., Chihara, K., Kimura, K., Fukata, Y., Nakamura, N., Matsuura, Y. and Kaibuchi, K. (1997). Formation of actin stress fibers and focal adhesions enhanced by Rho-kinase. *Science* **275**, 1308-1311.

Bertet, C., Sulak, L. and Lecuit, T. (2004). Myosin-dependent junction remodelling controls planar cell intercalation and axis elongation. *Nature* **429**, 667-671.

Blankenship, J. T., Backovic, S. T., Sanny, J. S., Weitz, O. and Zallen, J. A. (2006). Multicellular rosette formation links planar cell polarity to tissue morphogenesis. *Dev. Cell* **11**, 459-470.

Brand, A. H. and Perrimon, N. (1993). Targeted gene expression as a means of altering cell fates and generating dominant phenotypes. *Development* **118**, 401-415.

Brodu, V. and Casanova, J. (2006). The RhoGAP crossveinless-c links trachealess and EGFR signaling to cell shape remodeling in Drosophila tracheal invagination. *Genes Dev.* **20**, 1817-1828.

Brodu, V., Elstob, P. R. and Gould, A. P. (2004). EGF receptor signaling regulates pulses of cell delamination from the Drosophila ectoderm. *Dev. Cell* **7**, 885-895.

Brunner, D., Ducker, K., Oellers, N., Hafen, E., Scholz, H. and Klambt, C. (1994). The ETS domain protein pointed-P2 is a target of MAP kinase in the sevenless signal transduction pathway. *Nature* **370**, 386-389.

Campbell, G. (2002). Distalization of the Drosophila leg by graded EGF-receptor activity. *Nature* **418**, 781-785.

Costa, M., Wilson, E. T. and Wieschaus, E. (1994). A putative cell signal encoded by the folded gastrulation gene coordinates cell shape changes during Drosophila gastrulation. *Cell* **76**, 1075-1089.

Ettensohn, C. A. (1985). Gastrulation in the sea urchin embryo is accompanied by the rearrangement of invaginating epithelial cells. *Dev. Biol.* **112**, 383-390.

Faber, S. C., Dimanlig, P., Makarenkova, H. P., Shirke, S., Ko, K. and Lang, R. A. (2001). Fgf receptor signaling plays a role in lens induction. *Development* **128**, 4425-4438.

Gabay, L., Seger, R. and Shilo, B. Z. (1997a). In situ activation pattern of Drosophila EGF receptor pathway during development. *Science* **277**, 1103-1106.

Gabay, L., Seger, R. and Shilo, B. Z. (1997b). MAP kinase in situ activation atlas during *Drosophila* embryogenesis. *Development* **124**, 3535-3541.

Galindo, M. I., Bishop, S. A., Greig, S. and Couso, J. P. (2002). Leg patterning driven by proximal-distal interactions and EGFR signaling. *Science* **297**, 256-259.

Hardin, J. D. and Cheng, L. Y. (1985). The mechanisms and mechanics of archenteron elongation during sea urchin gastrulation. *Dev. Biol.* **115**, 490-501.

Hou, X. S., Chou, T. B., Melnick, M. B. and Perrimon, N. (1995). The torso receptor tyrosine kinase can activate Raf in a Ras-independent pathway. *Cell* **81**, 63-71.

Hutson, M. S., Tokutake, Y., Chang, M. S., Bloor, J. W., Venakides, S., Kiehart, D. P. and Edwards, G. S. (2003). Forces for morphogenesis investigated with laser microsurgery and quantitative modeling. *Science* **300**, 145-149.

Irvine, K. D. and Wieschaus, E. (1994). Cell intercalation during *Drosophila* germband extension and its regulation by pair-rule segmentation genes. *Development* **120**, 827-841.

Isaac, D. D. and Andrew, D. J. (1996). Tubulogenesis in Drosophila: a requirement for the trachealess gene product. *Genes Dev.* **10**, 103-117.

Kassis, J. A., Noll, E., VanSickle, E. P., Odenwald, W. F. and Perrimon, N. (1992). Altering the insertional specificity of a Drosophila transposable element. *Proc. Natl. Acad. Sci. USA* **89**, 1919-1923.

Kato, K., Chihara, T. and Hayashi, S. (2004). Hedgehog and Decapentaplegic instruct polarized growth of cell extensions in the *Drosophila* trachea. *Development* **131**, 5253-5261.

Keller, R. (2002). Shaping the vertebrate body plan by polarized embryonic cell movements. *Science* **298**, 1950-1954.

Keller, R., Davidson, L. A. and Shook, D. R. (2003). How we are shaped: the biomechanics of gastrulation. *Differentiation* **71**, 171-205.

Kiehart, D. P., Galbraith, C. G., Edwards, K. A., Rickoll, W. L. and Montague, R. A. (2000). Multiple forces contribute to cell sheet morphogenesis for dorsal closure in Drosophila. *J. Cell Biol.* **149**, 471-490.

Kosman, D., Small, S. and Reinitz, J. (1998). Rapid preparation of a panel of polyclonal antibodies to Drosophila segmentation proteins. *Dev. Genes Evol.* **208**, 290-294.

Ladher, R. K., Wright, T. J., Moon, A. M., Mansour, S. L. and Schoenwolf, G. C. (2005). FGF8 initiates inner ear induction in chick and mouse. *Genes Dev.* **19**, 603-613.

Leptin, M. and Grunewald, B. (1990). Cell shape changes during gastrulation in *Drosophila*. *Development* **110**, 73-84.

Llimargas, M. and Casanova, J. (1999). EGF signalling regulates cell invagination as well as cell migration during formation of tracheal system in Drosophila. *Dev. Genes Evol.* **209**, 174-179.

Manning, G. and Krasnow, M. A. (1993). Development of the *Drosophila* Tracheal System. In *The Development of Drosophila melanogaster* (ed. M. Bate and A. Martinez-Arias), pp. 2609-2686. New York: Cold Spring Harbor Laboratory Press.

Myat, M. M. and Andrew, D. J. (2000a). Fork head prevents apoptosis and promotes cell shape change during formation of the *Drosophila* salivary glands. *Development* **127**, 4217-4226.

Myat, M. M. and Andrew, D. J. (2000b). Organ shape in the Drosophila salivary gland is controlled by regulated, sequential internalization of the primordia. *Development* **127**, 679-691.

Oda, H. and Tsukita, S. (2001). Real-time imaging of cell-cell adherens junctions reveals that *Drosophila* mesoderm invagination begins with two phases of apical constriction of cells. *J. Cell Sci.* **114**, 493-501.

O'Neill, E. M., Rebay, I., Tjian, R. and Rubin, G. M. (1994). The activities of two Ets-related transcription factors required for Drosophila eye development are modulated by the Ras/MAPK pathway. *Cell* **78**, 137-147.

Parks, S. and Wieschaus, E. (1991). The Drosophila gastrulation gene concertina encodes a G alpha-like protein. *Cell* **64**, 447-458.

Raz, E. and Shilo, B. Z. (1993). Establishment of ventral cell fates in the Drosophila embryonic ectoderm requires DER, the EGF receptor homolog. *Genes Dev.* **7**, 1937-1948.

Ribeiro, C., Neumann, M. and Affolter, M. (2004). Genetic control of cell intercalation during tracheal morphogenesis in Drosophila. *Curr. Biol.* **14**, 2197-2207.
Royou, A., Sullivan, W. and Karess, R. (2002). Cortical recruitment of nonmuscle myosin II in early syncytial Drosophila embryos: its role in nuclear axial expansion and its regulation by Cdc2 activity. *J. Cell Biol.* **158**, 127-137.
Royou, A., Field, C., Sisson, J. C., Sullivan, W. and Karess, R. (2004). Reassessing the role and dynamics of nonmuscle myosin II during furrow formation in early Drosophila embryos. *Mol. Biol. Cell* **15**, 838-850.
Samakovlis, C., Hacohen, N., Manning, G., Sutherland, D. C., Guillemin, K. and Krasnow, M. A. (1996). Development of the *Drosophila* tracheal system occurs by a series of morphologically distinct but genetically coupled branching events. *Development* **122**, 1395-1407.
Schweitzer, R., Shaharabany, M., Seger, R. and Shilo, B. Z. (1995). Secreted spitz triggers the DER signalling pathway and is a limiting component in embryonic ventral ectoderm determination. *Genes Dev.* **9**, 1518-1529.
Shilo, B. Z. (2005). Regulating the dynamics of EGF receptor signaling in space and time. *Development* **132**, 4017-4027.
Simoes, S., Denholm, B., Azevedo, D., Sotillos, S., Martin, P., Skaer, H., Hombria, J. C. and Jacinto, A. (2006). Compartmentalisation of Rho regulators directs cell invagination during tissue morphogenesis. *Development* **133**, 4257-4267.
Sweeton, D., Parks, S., Costa, M. and Wieschaus, E. (1991). Gastrulation in *Drosophila:* the formation of the ventral furrow and posterior midgut invaginations. *Development* **112**, 775-789.
Tajiri, R., Tsuji, T., Ueda, R., Saigo, K. and Kojima, T. (2006). Fate determination of Drosophila leg distal regions by trachealess and tango through repression and stimulation, respectively, of Bar homeobox gene expression in the future pretarsus and tarsus. *Dev. Biol*. **303**, 461-473.
Tsuda, L., Inoue, Y. H., Yoo, M. A., Mizuno, M., Hata, M., Lim, Y. M., Adachi-Yamada, T., Ryo, H., Masamune, Y. and Nishida, Y. (1993). A protein kinase similar to MAP kinase activator acts downstream of the raf kinase in Drosophila. *Cell* **72**, 407-414.
Wappner, P., Gabay, L. and Shilo, B. Z. (1997). Interactions between the EGF receptor and DPP pathways establish distinct cell fates in the tracheal placodes. *Development* **124**, 4707-4716.
Wasserman, J. D. and Freeman, M. (1998). An autoregulatory cascade of EGF receptor signaling patterns the Drosophila egg. *Cell* **95**, 355-364.
Wilk, R., Weizman, I. and Shilo, B. Z. (1996). trachealess encodes a bHLH-PAS protein that is an inducer of tracheal cell fates in Drosophila. *Genes Dev.* **10**, 93-102.
Winter, C. G., Wang, B., Ballew, A., Royou, A., Karess, R., Axelrod, J. D. and Luo, L. (2001). Drosophila Rho-associated kinase (Drok) links Frizzled-mediated planar cell polarity signaling to the actin cytoskeleton. *Cell* **105**, 81-91.
Zallen, J. A. and Wieschaus, E. (2004). Patterned gene expression directs bipolar planar polarity in Drosophila. *Dev. Cell* **6**, 343-355.